

Gas Quantification Using Arrays of Intrinsic Zinc  
Oxide Thin Films Fabricated Using Three Different  
Successive Ionic Layer Adhesion and Reaction  
Processes

AMALLA, Bon Leif D.

January 29, 2019

# Contents

<b>List of Figures</b>	<b>ii</b>
<b>List of Figures</b>	<b>iii</b>
<b>1 Introduction</b>	<b>1</b>
1.1 Background of the Study . . . . .	1
1.2 Objectives of the Study . . . . .	3
1.3 Significance of the Study . . . . .	3
1.4 Scope and Limitations . . . . .	4
<b>2 Methodology</b>	<b>5</b>
2.1 Thin Film Fabrication . . . . .	5
2.2 Thin Film Characterization . . . . .	6
2.3 Model Creation . . . . .	7
2.3.1 Definition of microstructure functions . . . . .	7
2.3.2 Calculation of two-point spatial correlations . . . . .	7
2.3.3 Determination of optimal film orientation . . . . .	9
2.3.4 Determination of optimal microstructure function . . . . .	9
<b>References</b>	<b>10</b>

# List of Tables

2.1	Processing parameters manipulated and SILAR processes . . . . .	5
2.2	Summary of discrete microstructure functions . . . . .	8

# List of Figures

2.1	Basic orientation matrix . . . . .	6
2.2	Four point probe mechanism for determination of sheet resistance . . . . .	6

# Chapter 1

## Introduction

### 1.1 Background of the Study

Zinc oxide is a metal oxide semiconductor that has many different uses based on its structure such as in thin film electronics. Zinc oxide thin films are used in a wide variety of applications as gas sensors (Florido & Dagaas, 2017) and as photovoltaic cells (Saikumar, Skaria, & Sundaram, 2014). In order for the material to perform predictably, it is necessary to be able to correlate processing parameters to structural characteristics and property manifestations (Florido & Dagaas, 2017; Saikumar et al., 2014).

Due to the promise of rapid, high-throughput materials processing brought by data science driven approaches to materials processing through materials knowledge systems (MKS) frameworks (Gupta, Cecen, Goyal, Singh, & Kalidindi, 2015; Sun, Cecen, Gibbs, Kalidindi, & Voorhees, 2017; Yabansu, Patel, & Kalidindi, 2014) the field of materials informatics has grown.

There are several studies on computational simulations regarding material properties based on material structure and vice versa (Gupta et al., 2015; Yabansu et al., 2014).

The MKS framework, as defined by Yabansu et al. (2014), is dependent on the definition of a microstructure function  $m_r^n$ , representing the probability density of finding a specific local

state  $n \in N$ , characterized by physical and chemical properties, at a spatial bin  $r \in R$ . A number of studies have proposed the MKS to use discretized microstructure functions in order to apply statistical measures (Gupta et al., 2015; Sun et al., 2017; Yabansu et al., 2014). Numerous studies regarding the use of MKS frameworks have produced different microstructure functions depending on the application of the materials of interest ranging from two to ten and more local states (Gupta et al., 2015; Sun et al., 2017; Yabansu et al., 2014).

Property homogenization, within a probe volume, can be easily achieved through calculation and regression of calculated two point spatial correlations derived from assumptions of periodicity of the microstructure function in a given probe volume  $V$ . Research done by Sun et al. (2017) has shown that the assumption of periodicity of the microstructure function in a probe volume can make drastic computational improvements to the MKS compared to using finite element methods.

Currently, there exists an implementation of the MKS framework in the Python programming language (PyMKS) (Wheeler, Brough, Fast, Kalidindi, & Reid, 2014). The said framework implementation is maintained by researchers Georgia Institute of Technology and has been developed by a number of contributors to the repository. It is currently available on Github as an open-source project licensed under the MIT license.

As a rapidly growing computational language, Julia has proven to be more efficient and effective as other computational programming languages such as Matlab, Python (NumPy), and Octave (Bezanson, Edelman, S., & Shah, 2015). Examples of scientific applications are as a simulator for different systems dynamics through BioSimulator.jl (Landeros et al., 2018), for different quantum systems through QuantumOptics.jl (Krämer, Plankensteiner, Ostermann, & Ritsch, 2018), and modeling protein electrostatics using finite element methods through NESSie.jl (Kemmer, Rjasanow, & Hildebrandt, 2018).

## **1.2 Objectives of the Study**

The study aims to be able to define a new, simple microstructure function for the effective creation of MKS in developing material PSP linkages for the distribution of adhered particles of zinc oxide onto glass substrates. Specifically, the study will attempt to cover and discuss necessary measures that will aid in the creation of effective discrete spatial statistics of the particles, particle boundaries, and null spaces within the material structure, which will be used to find correlations to manipulations in the number of deposition cycles and annealing temperature.

The study also aims to be able to create a MKS methodology template in the Julia programming language. Specifically, the study aims to provide a new platform for materials informatics using the features of the programming language.

## **1.3 Significance of the Study**

Some of the numerous applications of zinc oxide thin films are dependent on the different distribution-dependent properties of the material, including thin film sheet resistance, porosity, and transmittance. The computational modeling of zinc oxide material structure with respect to processing parameters and properties is a significant milestone for the rapid, high-throughput production of precise application-specific materials.

The expression of the MKS framework, case-dependent or independent, in multiple languages allows for the growth of the framework into several applications allowing open source communities to further develop the capabilities of the framework.

## **1.4 Scope and Limitations**

The study mainly focuses on determining a family of microstructure functions that can be useful for building PSP linkages given sufficient material characterization. Since characterization is not readily accessible, structural characteristics used may be of low resolution. Thus, heavy caution must be observed in interpreting the results of the study.



# Chapter 2

## Methodology

### 2.1 Thin Film Fabrication

Thirty glass substrates, measuring  $1'' \times 0.25''$ , were cut from microscope slides. These substrates were subject to three successive ionic layer adhesion and reaction (SILAR) processes, S1, S2, and S3, as will be detailed in this section. All of the SILAR processes consist of a certain number of deposition cycles from a fixed precursor solution with  $0.095M$   $Zn^{2+}$  and  $0.190M$  NaOH and a thermal annealing at certain temperatures (Florido & Dagaas, 2017; Gao, Li, & Yu, 2004).

Table 2.1 summarizes the different SILAR processes along with the variations in processing parameters.

Table 2.1: Processing parameters manipulated and SILAR processes

—	S1	S2	S3
Deposition cycles	100	75	100
Annealing temperature	$450^{\circ}C$	$450^{\circ}C$	$500^{\circ}C$

1	3
2	4

Figure 2.1: Basic orientation matrix

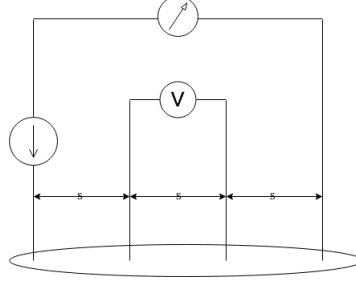


Figure 2.2: Four point probe mechanism for determination of sheet resistance

## 2.2 Thin Film Characterization

The fabricated thin films were characterized for determination of thin film structure and properties.

One thin film fabricated using each of the fabrication processes was chosen for optical microscopy. The fabricated material was split into four sections as shown in Figure 2.1. The sections were chosen such that the four corners of the rectangular substrate represent different probe volumes. The thin films were viewed under the high power objective lens ( $400\times$ ) of a digital compound microscope.

Overall thin film structure were also characterized with x-ray diffraction, using Cu-K $\alpha$  anode ( $\lambda = 1.54 \text{ \AA}$ ), and scanning electron microscopy at 20 kV.

Finally, the thin films sheet resistance values were derived from measurements from four-point probe sensing. The schematic for the four-point probe mechanism are shown in Figure 2.2.

## 2.3 Model Creation

### 2.3.1 Definition of microstructure functions

There are a total of 20 discrete microstructure functions (DMF) that are studied for the study. The definitions are divided into four categories depending on which of two axes will the DMFs be assumed to be periodic in. Each of the four categories contains five DMFs, which differ based on the method for determining the number of discrete local states within a certain probe volume  $V$ .

The functions can be summarized as Table 2.2. The dimensions of the probe volume  $V$  were chosen as odd products of small primes (2, 3, 5, and 7) to aid in the computation of two point spatial correlations, as will be discussed in the following subsection, with the exception of one function, with accounts for the dimensions of the size of a high resolution digital image.

### 2.3.2 Calculation of two-point spatial correlations

Two point spatial correlations are derived from optical microscopy images through the definition of the measures (Gupta et al., 2015).

$$m_r^{np} = \frac{1}{S_r N} \sum_{i=0}^N \sum_{j=0}^R m_r^p m_r^n$$

where  $n, p$  are the discrete local states of interest and  $r$  is the spatial bin of interest.

Image data were transformed into Julia 2D arrays (Bezanson et al., 2015) and further into a user defined data structure named *MaterialImage* which accounts for the parameters used for defining the DMFs (from the previous subsection). There are a total of 20 sets two point spatial correlations that will be considered.

Table 2.2: Summary of discrete microstructure functions

Periodic axes	Local states	Size of $V$
Both $i, j$	Two	$225 \times 225$
Both $i, j$	Two	$441 \times 441$
Both $i, j$	Three	$225 \times 225$
Both $i, j$	Three	$441 \times 441$
Both $i, j$	Three	$1920 \times 1080$
$j$	Two	$225 \times 225$
$j$	Two	$441 \times 441$
$j$	Three	$225 \times 225$
$j$	Three	$441 \times 441$
$j$	Three	$1920 \times 1080$
$i$	Two	$225 \times 225$
$i$	Two	$441 \times 441$
$i$	Three	$225 \times 225$
$i$	Three	$441 \times 441$
$i$	Three	$1920 \times 1080$
None	Two	$225 \times 225$
None	Two	$441 \times 441$
None	Three	$225 \times 225$
None	Three	$441 \times 441$
None	Three	$1920 \times 1080$

### 2.3.3 Determination of optimal film orientation

Since the preferred orientation of the fabrication of thin films is unknown, each of the three thin films have four hypothesized orientations based on circular permutations of the orientation matrix (Figure 2.1).

For each of the calculated two point spatial correlations, the values will undergo principal component analysis to obtain the orthogonal latent descriptors (Gupta et al., 2015; Sun et al., 2017). This is done with *MultivariateStats.jl*, a package available for multivariate statistical analysis (Dahua, 2018). Optimal orientation is determined when the variance of the dimensionally-reduced two point statistics, *i.e.* *the matrix trace of the covariance matrix* is minimized.

### 2.3.4 Determination of optimal microstructure function

The plots for the two-point statistics are manually compared. Partial least squares analysis (PLSA) is done to compare the ability of the DMF to capture the variation of derived sheet resistance values. Evaluation of the optimal microstructure function will be based on the following parameters:

1. Variance capture via PLSA
2. Qualitative assessment of clustering of microstructure ensembles

# References

- Bezanson, J., Edelman, A., S., K., & Shah, V. B. (2015). Julia: A fresh approach to numerical computing. *Society for Industrial and Applied Mathematics*, 59, 65–98.
- Dahua, L. (2018). Multivariatestats documentation [Computer software manual]. Retrieved 24 Jan 2018, from [media.readthedocs.org/pdf/multivariatestatsjl/latest/multivariatestatsjl.pdf](http://media.readthedocs.org/pdf/multivariatestatsjl/latest/multivariatestatsjl.pdf)
- Florido, E. A., & Dagaas, N. A. C. (2017). Carbon monoxide gas sensing using zinc oxide deposited by successive ionic layer adhesion and reaction. *IOP Conf. Series: Materials Science and Engineering*, 201.
- Gao, X. D., Li, X. M., & Yu, W. D. (2004). Synthesis and optical properties of zno nanocluster porous films deposited by modified silar method. *Applied Surface Science*, 229, 275–281.
- Gupta, A., Cecen, A., Goyal, S., Singh, A. K., & Kalidindi, S. R. (2015). Structure-property linkages using a data science approach: Application to a non-metallic inclusion/steel composite system. *Acta Materialia*, 91, 239–254.
- Kemmer, T., Rjasanow, S., & Hildebrandt, A. (2018). Essie.jl: Efficient and intuitive finite element and boundary element methods for nonlocal protein electrostatics in the julia language. *Journal of Computational Science*, 28, 193–203.
- Krämer, S., Plankensteiner, D., Ostermann, L., & Ritsch, H. (2018). Quantumoptics.jl: A julia framework for simulating open quantum systems. *Computer Physics Communications*, 227, 109–116.
- Landeros, A., Stutz, T., Keys, K. L., Alekseyenko, A., Sinsheimer, J. S., Lange, K., & Sehl, M. E. (2018). Biosimulator.jl: Stochastic simulation in julia. *Computer Programs and Methods in Biomedicine*, 167, 23–35.
- Saikumar, A. K., Skaria, G., & Sundaram, K. B. (2014). Zno gate based mosfets for sensor applications. *ECS Transactions*, 61, 65–69.
- Sun, Y., Cecen, A., Gibbs, J. W., Kalidindi, S. R., & Voorhees, P. W. (2017). Analytics on large microstructure datasets using two-point spatial correlations: Coarsening of dendritic structures. *Acta Materialia*, 132, 374–388.
- Wheeler, D., Brough, D., Fast, T., Kalidindi, S., & Reid, A. (2014). *Pymks: Materials knowledge system in python*.
- Yabansu, Y. C., Patel, D. K., & Kalidindi, S. R. (2014). Calibrated localization relationships for elastic response of polycrystalline aggregates. *Acta Materialia*, 81, 151–160.